

# Unsupervised Learning of Debiased Representations with Pseudo-Attributes

Seonguk Seo<sup>1</sup>   Joon-Young Lee<sup>2</sup>   Bohyung Han<sup>1</sup>

<sup>1</sup>Seoul National University   <sup>2</sup>Adobe Research

{seonguk, bhhan}@snu.ac.kr   jolee@adobe.com

## Abstract

*Dataset bias is a critical challenge in machine learning, and its negative impact is aggravated when models capture unintended decision rules with spurious correlations. Although existing works often handle this issue using human supervision, the availability of the proper annotations is impractical and even unrealistic. To better tackle this challenge, we propose a simple but effective debiasing technique in an unsupervised manner. Specifically, we perform clustering on the feature embedding space and identify pseudo-attributes by taking advantage of the clustering results even without an explicit attribute supervision. Then, we employ a novel cluster-based reweighting scheme for learning debiased representation; this prevents minority groups from being discounted for minimizing the overall loss, which is desirable for worst-case generalization. The extensive experiments demonstrate the outstanding performance of our approach on multiple standard benchmarks, which is even as competitive as the supervised counterpart.*

## 1. Introduction

Deep neural networks have achieved impressive performance by minimizing the average loss on training datasets. Although we typically adopt the empirical risk minimization framework as a training objective, it is sometimes problematic due to dataset bias leading to significant degradation of worst-case generalization performance as discussed in [2, 35, 17, 11, 36]. This is because models do not always learn what we expect, but, to the contrary, rather capture unintended decision rules with spurious correlations. For example, on the Colored MNIST dataset [20, 24, 1], where each digit is highly correlated to a certain color, a network often learns the patterns given by the color of each image, not the digit information while ignoring few conflicting samples. Such an unintended rule works well on most of training samples, but gives unexpected worst-case errors for subpopulation samples, which makes the model unable to generalize on unseen test environments with distribution shifts or robustness criteria. Figure 1 illustrates the problem

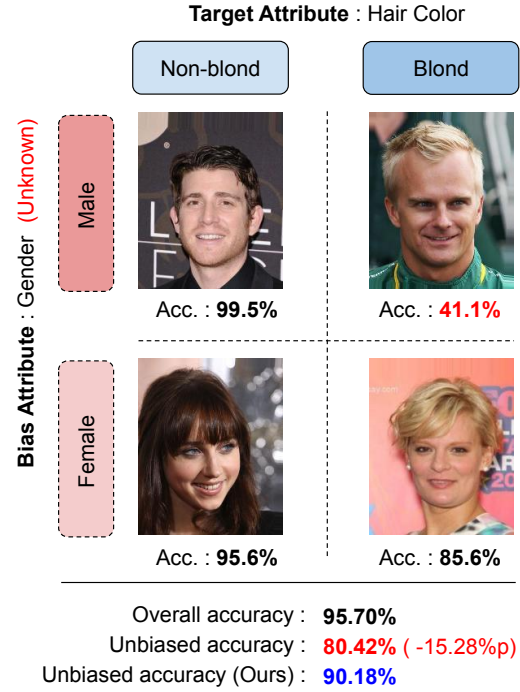


Figure 1: Representative examples on the CelebA dataset for the problem that we focus on. Since most of the people with blond hair are women, *hair color* attribute has a spurious correlation with *gender* attribute. Thus, when trained to classify the *hair color*, a network captures the unintended decision rule using *gender*, leading to poor worst-group and unbiased accuracies, despite its high overall accuracy. Our model aims to learn debiased representation, which gives better worst-group and unbiased accuracies, especially when the bias information is unavailable.

that we mainly deal with in this paper.

To mitigate the bias issue, learning debiased representations from a biased dataset has received growing attention from machine learning community [20, 32, 25, 13, 1, 3]. However, most previous works assume the explicit supervision as well as the presence of the dataset bias. This assumption is not practical because identifying what forms of

bias exist or which attributes have spurious correlations requires thorough analysis of a dataset. In addition, even if we have prior knowledge about the bias, the relevant annotations over all training examples require laborious efforts. Contrary to the supervised approaches, [24, 28] tackle a more challenging setting, where the bias information is unavailable, via failure-based learning and subgroup-based penalizing, respectively.

This paper presents a simple but effective dataset debiasing technique based on unsupervised clustering via feature embedding. We first observe that the representations of the examples in target and bias attributes are highly correlated in the feature space in a biased model after training for a sufficient number of epochs. Based on this observation, we identify *bias* pseudo-attributes from the clustering results within each class, without any bias supervision. To exploit the bias pseudo-attributes for learning debiased representations, we introduce a reweighting scheme for the corresponding clusters, where each cluster has an importance weight depending on its size and accuracy. This strategy encourages the minority clusters to participate in the optimization process actively, which is critical to improve the worst-group generalization. Despite its simplicity, our method turns out to be very effective for debiasing without any supervision of the bias information; it is even comparable to the supervised debiasing method.

The main contributions of our work are summarized as follows.

- We propose a simple but effective unsupervised debiasing approach, which requires no explicit supervision about spurious correlations across attributes.
- We introduce a technique to learn debiased representations by identifying pseudo-attributes via clustering and weighting the corresponding clusters based on both their size and target loss.
- We provide extensive experimental results and achieve outstanding performance in terms of unbiased and worst-group accuracies, which are even as competitive as supervised debiasing methods.

The rest of the paper is organized as follows. We review the prior research in Section 2. Section 3 presents our proposed framework for learning debiased representation, and Section 4 demonstrates its effectiveness with extensive analysis. We conclude our paper in Section 5.

## 2. Related Work

### 2.1. Bias in computer vision tasks

Real-world datasets contain inevitable biases due to their insufficiently controlled collection process, and consequently, deep neural networks often capture unintended

correlations between the true labels and the spuriously correlated ones. Measuring and mitigating the potential risks posed by dataset or algorithmic bias has been extensively investigated in various computer vision tasks [29, 20, 15, 31, 3, 34]. For example, some VQA models often take advantage of statistical regularities between answer occurrences and certain patterns of questions without using the visual features at all [3, 6]. To prevent using undesirable correlation in biased datasets, existing approaches often rely on human supervision for bias annotations and present several technical directions such as data augmentation [12, 37], model ensembles [3, 6], and statistical properties [1]. Such supervised debiasing techniques have been applied to various computer vision tasks by exploiting known application-specific bias information, including uni-modality of dataset in visual question answering [3], stereotype textures in image recognition [12], temporal invariance in action recognition [19], and demographic information in facial image recognition [25, 37, 33].

### 2.2. Handling distribution shifts

Distributional shift has recently emerged as a critical challenge in machine learning, where the goal of the optimization is to learn a robust model in a test environment with the shifts. Distributionally robust optimization (DRO) [2, 10, 8, 16] has been proposed to improve the worst-case generalization performance over potential test distributions, and has provided theoretical background of Group DRO [25] and its variation [28]. However, the objective of DRO often leads to an overly conservative model and results in performance degeneration on unseen environments [9, 14]. To construct a more realistic uncertainty set of test distributions, some approaches pose additional assumptions. One popular assumption is that training examples are provided in groups, and the uncertainty set is represented by a mixture of these groups. This assumption is also used in robust federated learning [23, 18], algorithmic fairness [35, 5, 7], and domain generalization [17, 4, 27]. Our framework also handles the group shifts under this assumption, but does not rely on the supervision of group information.

### 2.3. Debiasing via loss-based reweighting

There exist several generic debiasing approach based on sample weighting with observed losses under different supervision levels [25, 24, 28]. Sagawa *et al.* [25] adopt the supervised bias information to define groups and tackle the worst-case generalization among the groups, while recent works [24, 28] tackle a more challenging unsupervised setting, where the bias information is unavailable. Group DRO [25] exploits the group information specified by the bias attributes and improves the worst-group generalization performance. On the other hand, Nam *et al.* [24] em-

ploy the difference between the generalized and standard cross-entropy loss to capture the bias-alignment for sample weighting while Sohoni *et al.* [28] estimate subclass labels via clustering techniques and use the information for distributionally robust optimization to mitigate hidden stratification. Although the unsupervised approaches work well in small and artificial datasets such as MNIST, their performance improvement is marginal in real-world datasets like as CelebA. Our framework also belongs to unsupervised methods that do not use the bias information to learn debiased representations.

### 3. Method

This section discusses the proposed debiasing approach based on pseudo-attribute identification and sample weighting motivated by our observation about bias attributes.

#### 3.1. Preliminaries

Let an example  $\mathbf{x}$  be associated with a set of  $m$  latent attributes  $\mathcal{A} := \{a_1, \dots, a_m\}$ . The goal of our model is to predict a target attribute  $a_t \in \mathcal{A}$  by estimating the intended causation  $p(a_t|\mathbf{x})$ , which does not involve any undesirable correlation to other attributes, *i.e.*,  $p(a_t|\mathbf{x}) = p(a_t|\mathbf{x}, a_i)$ ,  $\forall a_i \in \mathcal{A} - \{a_t\}$ . On the other hand, spurious correlation indicates strong coincidence between two attributes  $a_i, a_j \in \mathcal{A}$ , *i.e.*,  $H(a_i|a_j) \approx 0$ , which have no causal relationship between them. The algorithmic bias means that a bias attribute  $a_b \in \mathcal{A}$  has a spurious correlation to  $a_t$  and affects the prediction to  $a_t$ , *i.e.*,  $p(a_t|\mathbf{x}) \neq p(a_t|\mathbf{x}, a_b)$ . A group is defined by a set of target and bias attributes, *e.g.*,  $g = (a_t, a_b)$ .

#### 3.2. Observation

If a bias attribute is highly correlated to a target attribute while being easy to learn, the model may ignore few conflicting examples and learn its decision rule based on the bias attributes with spurious correlations to maximize accuracy [24, 26]. To prevent this undesirable situation, a simple group balancing upweighting or subsampling strategies [26] are known to be effective while they do not work well with realistic scenarios, where the bias information is not available during training.

To overcome this challenge, from our intuition, we analyze the feature semantics over the target and bias attributes. We first naïvely train a base model on the CelebA dataset to classify *heavy makeup*, and visualize the representation of the examples after convergence with a sufficient number of epochs ( $T = 100$ ). We select *gender* as a bias attribute, but do not utilize any information of the bias attribute during training. It turns out that, even without using the bias information during training, the examples drawn from certain groups, which are given by a combination of hair color

and gender attribute values in this case, *e.g.*, (male, non-blond) and (female, blond), are located closely in the feature space. This observation implies that it is possible to identify bias pseudo-attributes by taking advantage of the embedding results even without attribute supervisions. Our unsupervised debiasing framework is based on the capability to identify the bias pseudo-attributes via clustering.

#### 3.3. Formulation

Suppose that training examples,  $(\mathbf{x}, y)$ , are drawn from a certain distribution  $\tilde{P}$ . Given a loss function  $\ell(\cdot)$  and model parameters  $\theta$ , the objective of the empirical risk minimization (ERM) is to optimize the following expected loss:

$$\min_{\theta} \mathbb{E}_{(\mathbf{x}, y) \sim P} [\ell((\mathbf{x}, y); \theta)], \quad (1)$$

where  $P$  is the empirical distribution over training data that approximates the true distribution  $\tilde{P}$ . Although ERM generally works well, it tends to ignore minority examples in correlated groups conflicting with bias attributes and implicitly assumes the consistency of the underlying distributions for training and testing data. Consequently, the approach often leads to high unbiased and worst-group test error [8, 25].

Several distributionally robust optimization (DRO) techniques [2, 8, 16] can be employed to tackle the dataset bias and distribution shift problems and maximize unbiased generalization accuracy. They consider a particular uncertainty set  $\mathcal{Q}_P$ , which is close to the training distribution  $P$ , *e.g.*,  $\mathcal{Q}_P = \{Q : D_f[Q||P] \leq \delta\}$ , where  $D_f[\cdot||\cdot]$  indicates an  $f$ -divergence function<sup>1</sup>. To minimize the worst-case loss over the uncertainty distribution  $\mathcal{Q}_P$ , DRO optimizes

$$\min_{\theta} \left\{ \mathbb{R}(\theta) := \sup_{Q \in \mathcal{Q}_P} \mathbb{E}_{(\mathbf{x}, y) \sim Q} [\ell((\mathbf{x}, y); \theta)] \right\}. \quad (2)$$

However, this objective makes the model overly pessimistic and leads to considering even the implausible worst cases [9, 14].

The group distributionally robust optimization, referred to as group DRO [25] constructs more realistic sets of test distributions by leveraging the prior knowledge of group information. They assume the training distribution  $P$  is a mixture of  $G$  groups,  $P_g$ , which is given by

$$P_g = \sum_{g \in \mathcal{G}} c_g P_g, \quad c \in \Delta_G \quad (3)$$

where  $\mathcal{G} = \{1, \dots, G\}$  and  $\Delta_G$  is a  $(G - 1)$ -dimensional simplex. Then the uncertainty set  $\mathcal{Q}_P$  is defined by a set of all possible mixtures of these groups, *i.e.*,  $\mathcal{Q}_{P_g} = \{\sum_{g \in \mathcal{G}} c_g P_g : c \in \Delta_G\}$ . Because  $\mathcal{Q}_{P_g}$  is a simplex, its

<sup>1</sup>Let  $P$  and  $Q$  be probability distributions over a space  $\Omega$ , then  $f$ -divergence is  $D_f(P||Q) = \int_{\Omega} f(\frac{dP}{dQ}) dQ$ .

optimum is achieved at a vertex, thus minimizing the worst-case risk of  $\mathcal{Q}_{P_G}$  is equivalent to

$$\min_{\theta} \left\{ \mathbb{R}_G(\theta) := \max_{g \in \mathcal{G}} \mathbb{E}_{(\mathbf{x}, y) \sim P_g} [\ell((\mathbf{x}, y); \theta)] \right\}. \quad (4)$$

Different from the group DRO setting, we do not know the group assignments for each training samples. Instead, we use the pseudo-attribute information, obtained by any clustering algorithm in the feature embedding space, to define groups. Note that the clustering is performed with the representations given by the base model trained with no debiasing, which is parameterized with  $\tilde{\theta}$ . Our goal is to minimize dataset bias and maximize unbiased accuracy, and we need to consider all groups for optimization. Since each cluster has different importance weight, we provide individual groups with soft weights to compute the expected loss. Then, the final objective of our framework is given by minimizing a weighted empirical risk as follows:

$$\min_{\theta} \left\{ \mathbb{R}_K(\theta) := \mathbb{E}_{(\mathbf{x}, y) \sim P} \left[ \omega_{h((\mathbf{x}, y); \tilde{\theta})} \ell((\mathbf{x}, y); \theta) \right] \right\}, \quad (5)$$

where  $\omega_{h((\mathbf{x}, y); \tilde{\theta})}$  denotes the weight of the cluster that the example  $(\mathbf{x}, y)$  belongs to<sup>2</sup>. The details of the weight assignment will be discussed next.

### 3.4. Sample weighting with pseudo-attributes

Based on our observation described in Section 3.2, we first cluster training examples in each class on the feature embedding space defined by the base model optimized sufficiently, *e.g.*, for 100 epochs using a naïve classification loss. We suppose that each cluster corresponds to a pseudo-attribute. Among all the clusters, we attempt to focus on the samples in the minority clusters, especially when they have high average loss. So, a common failure case in the presence of dataset bias is incurred by ignoring specific subpopulation groups for minimizing the overall training loss.

This intuition implies that minority clusters are prone to be ignored due to its scale. A cluster may contain the examples conflicting with bias attributes, which is problematic since it will have high losses and thus result in poor generalization performance. If the minority clusters consist of mostly bias-aligned samples, they will apparently achieve high classification accuracy while the examples in the clusters are actually ignored during training. Therefore, to handle dataset bias issue, we should consider both scale and average difficulty (loss) of each cluster, unlike group DRO [25] and George [28], which focus only on the average loss. To this end, we calculate the importance of each

<sup>2</sup> $h((\mathbf{x}, y); \tilde{\theta}) = k$  denotes that the example  $(\mathbf{x}, y)$  is assigned to the  $k^{\text{th}}$  cluster, based on the features extracted from the base model, parameterized by  $\tilde{\theta}$ .

---

#### Algorithm 1: Optimization procedure

---

```

1 Require: step size  $\eta_\theta$ , momentum  $m$ , training steps
    $T$ , batch size  $B$ , the number of clusters  $K$ 
2 Base model:
3 Initialize  $\tilde{\theta}$ 
4 for  $t = 1, \dots, T$  do
5   Sample  $(\mathbf{x}_i, y_i) \sim P$  for  $i = 1, \dots, B$ ;
6    $\tilde{\theta} \leftarrow \tilde{\theta} - \eta_{\tilde{\theta}} \sum_{i=1}^B \nabla \ell((\mathbf{x}_i, y_i); \tilde{\theta})$ ;
7 end
8  $P_k = \{(\mathbf{x}_n, y_n) \mid h((\mathbf{x}_n, y_n); \tilde{\theta}) = k \text{ for all } n\}$ ;
9  $N_k = |P_k|$ ;
10 Target model:
11 Initialize  $\theta$  and  $\omega_k$  for  $k = 1, \dots, K$ 
12 for  $t = 1, \dots, T$  do
13    $\omega_k \leftarrow (1 - m)\omega_k + \frac{m}{N_k} \mathbb{E}_{(\mathbf{x}, y) \sim P_k} [\ell((\mathbf{x}, y); \theta)]$ 
14   for  $k = 1, \dots, K$ ;
15   Sample  $(\mathbf{x}_i, y_i) \sim P$  for  $i = 1, \dots, B$ ;
16    $k_i = h((\mathbf{x}_i, y_i); \tilde{\theta})$ ;
17    $\bar{\omega}_{k_i} = \omega_{k_i} / \sum_{i=1}^B \omega_{k_i}$ ;
18    $\theta \leftarrow \theta - \eta_\theta \sum_{i=1}^B \bar{\omega}_{k_i} \nabla \ell((\mathbf{x}_i, y_i); \theta)$ ;
19 end

```

---

cluster in our reweighting scheme to train the target model as follows:

$$\begin{aligned} \omega_k &= \frac{\mathbb{E}_{(\mathbf{x}, y) \sim P_k} [\ell((\mathbf{x}, y); \theta)]}{N_k} \\ &= \frac{\mathbb{E}_{(\mathbf{x}, y) \sim P} [\ell((\mathbf{x}, y); \theta) \mid h((\mathbf{x}, y); \tilde{\theta}) = k]}{\sum_i \mathbb{1}(h((\mathbf{x}_i, y_i); \tilde{\theta}) = k)} \end{aligned} \quad (6)$$

where  $\theta$  and  $\tilde{\theta}$  indicates the parameters of the final and base models, respectively,  $h(\cdot)$  is a cluster membership function, and  $\mathbb{1}(\cdot)$  is an indicator function. Note that  $P_k$  denotes the sample distribution of the  $k^{\text{th}}$  cluster and  $N_k$  is the number of samples in the  $k^{\text{th}}$  cluster, where  $k \in \mathcal{K} = \{1, \dots, K\}$ .

### 3.5. Algorithm procedure

Algorithm 1 presents the optimization procedure of the proposed framework. We first naïvely train a baseline network (Line 4-7), parameterized by  $\tilde{\theta}$ , and cluster all training examples based on the feature representations from the network to obtain the membership distribution  $P_k$  and the size of cluster  $N_k$  (Line 8-9). Based on the cluster assignments, we calculate the importance weight of each cluster  $\omega_k$  using the target model, parameterized by  $\theta$ , where the weight is updated by exponential moving average at each iteration (Line 13). We finally use the normalized importance weight over a mini-batch to train the target model (Line 17).



Table 1: Unbiased and worst-group results in the existence of spurious correlation between target and bias attributes on the test split of the CelebA dataset. LfF\* denotes a variant of LfF [24], which fine-tuned only the classification layer of a trained baseline model, for additional comparison to ours. All experimental results are the average of three runs.

Target	Bias	Unbiased accuracy (%)					Worst-group accuracy (%)				
		Unsupervised				Supervised	Unsupervised				Supervised
		Base	LfF	LfF*	Ours	Group DRO	Base	LfF	LfF*	Ours	Group DRO
Blond Hair	Gender	80.42	59.46	84.89	<b>90.18</b>	<b>91.39</b>	41.02	34.23	57.96	<b>82.54</b>	<b>87.86</b>
Heavy Makeup	Gender	71.19	56.34	71.85	<b>73.78</b>	<b>72.70</b>	17.35	<b>30.81</b>	23.87	<b>39.84</b>	21.36
Pale Skin	Gender	71.50	78.69	75.23	<b>90.06</b>	<b>90.55</b>	36.64	57.38	43.26	<b>88.60</b>	<b>87.68</b>
Wearing Lipstick	Gender	73.90	53.79	73.84	<b>78.28</b>	<b>78.26</b>	31.38	25.52	31.92	<b>46.52</b>	<b>46.08</b>
Young	Gender	78.19	45.99	79.58	<b>82.27</b>	<b>82.40</b>	52.79	0.34	57.79	<b>74.33</b>	<b>76.29</b>
Double Chin	Gender	64.61	65.46	68.47	<b>82.92</b>	<b>83.19</b>	21.33	28.19	28.24	<b>67.78</b>	<b>72.94</b>
Chubby	Gender	67.42	60.03	71.56	<b>83.88</b>	<b>81.90</b>	24.30	7.60	34.09	<b>72.32</b>	<b>72.64</b>
Wearing Hat	Gender	93.53	84.56	94.81	<b>96.80</b>	<b>96.84</b>	85.12	69.06	88.31	<b>94.94</b>	<b>94.67</b>
Oval Face	Gender	62.70	57.64	62.30	<b>67.18</b>	<b>65.40</b>	29.15	7.40	36.00	<b>55.78</b>	<b>56.84</b>
Pointy Nose	Gender	62.10	42.20	63.83	<b>68.90</b>	<b>70.71</b>	25.80	1.05	38.04	<b>52.48</b>	<b>63.76</b>
Straight Hair	Gender	70.28	39.57	72.84	<b>79.18</b>	<b>77.04</b>	47.82	1.95	58.53	<b>72.09</b>	<b>66.10</b>
Blurry	Gender	73.05	76.70	77.52	<b>88.93</b>	<b>87.05</b>	45.68	43.81	52.35	<b>84.10</b>	<b>82.06</b>
Narrow Eyes	Gender	63.18	68.53	67.77	<b>76.39</b>	<b>76.72</b>	27.01	31.81	38.53	<b>73.24</b>	<b>71.47</b>
Arched Eyebrows	Gender	69.72	56.17	71.87	<b>74.77</b>	<b>78.30</b>	34.76	26.21	44.97	<b>54.36</b>	<b>69.44</b>
Bags Under Eyes	Gender	69.47	44.61	71.86	<b>77.84</b>	<b>75.88</b>	41.65	0.06	49.10	<b>62.55</b>	<b>63.34</b>
Bangs	Gender	89.04	41.41	89.04	<b>93.94</b>	<b>94.45</b>	76.91	3.18	82.37	<b>92.21</b>	<b>92.12</b>
Big Lips	Gender	60.87	46.74	62.15	<b>66.50</b>	<b>63.70</b>	30.85	31.44	38.54	<b>56.99</b>	<b>47.55</b>
No Beard	Gender	73.11	60.12	73.13	<b>79.58</b>	<b>77.86</b>	13.30	11.92	20.00	<b>40.00</b>	<b>36.70</b>
Receding Hairline	Gender	69.72	70.57	74.58	<b>84.95</b>	<b>85.15</b>	35.69	32.10	45.53	<b>79.11</b>	<b>79.12</b>
Wavy Hair	Gender	73.10	48.00	74.53	<b>79.89</b>	<b>79.65</b>	38.01	0.06	45.24	<b>65.74</b>	<b>66.79</b>
Wearing Earrings	Gender	72.17	59.35	74.17	<b>84.57</b>	<b>83.50</b>	26.26	0.10	32.95	<b>72.81</b>	<b>75.24</b>
Wearing Necklace	Gender	55.04	58.64	57.21	<b>68.96</b>	<b>62.89</b>	2.72	0.22	6.67	<b>41.93</b>	<b>24.34</b>
<b>Average</b>	Gender	72.67	58.65	74.87	<b>81.74</b>	<b>80.87</b>	39.91	21.91	47.88	<b>69.84</b>	<b>69.68</b>

## 4. Experiments

This section presents our experimental results to demonstrate the effectiveness of the proposed framework. We compare the proposed approach with existing methods and analyze the characteristics of our sample weighting strategy via comprehensive ablation study.

### 4.1. Dataset

CelebA [21] is a large-scale face dataset for face image recognition, containing 40 attributes for each image. Following the previous works [25, 24], we primarily examine two attributes, *hair color* and *heavy makeup*, both of which *gender* attribute is spuriously correlated to. We set hair color and heavy makeup as the target attributes, and gender as the bias attribute. For more comprehensive results, we also analyze the other 32 attributes as the target attributes.

Waterbirds [25] is a synthesized dataset with 4,795 training examples, which are created by combining birds photographs from the Caltech-UCSD Birds-200-2011 (CUB) dataset [30] and background images borrowed from the Places dataset [38]. The two attributes—one is the type of bird, {waterbird, landbird} and the other is background places, {water, land}, are used for the experiments with this dataset.

The Colored-MNIST dataset [20, 24, 1] is an extension of MNIST with the color attributes, where each digit is highly correlated to a certain color. There are 60,000 training examples and 10,000 test examples, where the ratio of bias-aligned samples<sup>3</sup> is 95%. We follow the protocol of [24] for the experiment.

### 4.2. Implementation details

For CelebA and Waterbirds, we use a ResNet-18 as our backbone network, which is pretrained on ImageNet. We train our model using the Adam optimizer with a learning rate of  $1 \times 10^{-4}$ , a batch size of 256, and a weight decay rate of 0.01. For the Colored MNIST dataset, we adopt a multi-layer perceptron with three hidden layers, each of which has 100 hidden units. We also employ the same Adam optimizer with a learning rate of  $1 \times 10^{-3}$ . We train the models for 100 epochs for all experiments, and decay the learning rate using a cosine annealing [22].

For clustering, we extract features from a separately trained base network with the standard classification loss and perform  $k$ -means clustering with  $K = 8$  in all experiments. The cluster weight of the  $k^{\text{th}}$  cluster,  $w_k$ , is updated

<sup>3</sup>It denotes the samples that are correctly classified by using the bias attribute (color).

Table 2: Unbiased and worst-group results on the Waterbirds dataset.

Target	Bias	Unbiased accuracy (%)					Worst-group accuracy (%)				
		Unsupervised				Supervised Group DRO	Unsupervised				Supervised Group DRO
		Base	LfF	LfF*	Ours		Base	LfF	LfF*	Ours	
Object	Place	84.63	85.48	84.57	<b>87.05</b>	<b>88.99</b>	62.39	68.02	61.68	<b>71.39</b>	<b>80.82</b>
Place	Object	87.99	85.77	85.05	<b>88.44</b>	<b>89.20</b>	73.34	62.37	60.00	<b>79.16</b>	<b>85.27</b>

Table 3: Unbiased accuracy (%) on the valid split of the Colored-MNIST dataset.

Target	Bias	Unsupervised			Supervised Group DRO
		Baseline	LfF	Ours	
Digit	Color	74.48	85.15	<b>85.26</b>	<b>85.88</b>
Color	Digit	<b>99.95</b>	<b>99.91</b>	99.82	98.96

by exponential moving average at each iteration with a momentum  $m$  of 0.3. All the results reported in our paper are obtained from the average of three runs.

### 4.3. Evaluation protocol

To evaluate the unbiased accuracy with an imbalanced evaluation set, we measure the accuracy of each group ( $a_t$ ,  $a_b$ ), where  $a_t$  and  $a_b$  denotes the indices of target and bias attributes, respectively. We report the average accuracy of each target and bias attribute pair as in [24]. We also test the worst-group accuracy among all groups to compare the debiasing performance of the proposed algorithm with other methods.

### 4.4. Results

**CelebA** Before evaluating our frameworks, we first thoroughly analyze the CelebA dataset in terms of algorithmic bias among the attributes. There are a total of 40 attributes in the CelebA dataset. For simplicity, the bias attribute is fixed to *gender*, and we analyze the relation to the targets given by other 39 attributes. We select the target attributes that have at least 10 images in the test split, for the reliable evaluation results<sup>4</sup>. We suppose that the algorithmic bias exists between target and bias attributes when a baseline model gives a large performance gap between its overall accuracy and unbiased accuracy (*e.g.*,  $>5\%$  points). We found that 26 out of 32 attributes have spurious correlation to gender, and report the results for the attributes. See our supplementary files for more detailed analysis.

Table 1 presents the experimental results of the proposed algorithm on the CelebA dataset, in comparison to the existing methods as well as the baseline model. Our model significantly outperforms the baseline and LfF [24] for all target attributes on both unbiased and worst-group accu-

cies. Note that our model is almost competitive to a supervised approach, Group DRO [25], without the explicit bias information. On the other hand, we observe that training the model with LfF deteriorates performance even compared to the baseline. This is because it fixes the feature extractor and only trains its classifier at the end of the network<sup>5</sup>. To conduct a meaningful comparison with stable results, we first train the baseline model used in our experiment for 100 epochs and then fine-tune the classification layer only based on the LfF algorithm; this version is referred to as LfF\* in the rest of this section. Although the performance of LfF\* is stable, the improvement by debiasing is still limited compared to Group DRO and our approach. Additional experimental results with various bias attributes are provided in our supplementary documents.

**Waterbirds** We also evaluate our model on the Waterbirds dataset and present the results in Table 2. As in the CelebA dataset, our model achieves the best accuracies among the unsupervised methods on both the unbiased and worst-group evaluation, and comparable results from the supervised method [25]. The results on Waterbirds imply that our model is robust to small-scale datasets as well.

**Colored-MNIST** Table 3 shows that our model achieves consistent accuracy in the digit classification with color bias. In addition, the color classification performance turns out to be also competitive to the baseline when the algorithmic bias does not exist while the supervised approach is not good at this setting.

### 4.5. Analysis

**Results with no algorithmic bias** We test our algorithm on unbiased datasets to make sure that it is dependable on the cases without algorithmic bias. The unbiased setting is defined by the configuration that a baseline model involves a marginal difference between its overall accuracy and unbiased accuracy (*e.g.*,  $< 5\%$  points). Similar to Table 1, we identify a subset of target attributes in CelebA, which is not spuriously correlated to gender; there exist 6 out of 32 attributes. Table 4 illustrates the results of the 6 target attributes, where the accuracies of our approach is most consistent among the 4 methods. This implies that our frame-

<sup>4</sup>The removed target attributes are 5 o'clock shadow, bald, rosy cheeks, sideburns, goatee, mustache and wearing necktie.

<sup>5</sup><https://github.com/alinelab/LfF>

Table 4: Unbiased and worst-group results on the CelebA dataset with the target attributes where the algorithmic bias does not exist.

Target	Bias	Unbiased accuracy (%)					Worst-group accuracy (%)				
		Unsupervised				Supervised Group DRO	Unsupervised				Supervised Group DRO
		Base	LfF	LfF*	Ours		Base	LfF	LfF*	Ours	
Attractive	Gender	76.05	30.18	75.97	<b>77.90</b>	<b>78.35</b>	63.61	6.09	64.78	<b>65.20</b>	<b>66.30</b>
Smiling	Gender	91.66	74.62	91.20	<b>92.08</b>	<b>91.64</b>	88.49	60.09	<b>88.65</b>	<b>90.06</b>	88.48
Mouth Open	Gender	93.10	81.85	92.96	<b>93.45</b>	<b>93.64</b>	91.52	66.92	<b>92.44</b>	<b>92.27</b>	91.69
High Cheekbones	Gender	83.44	48.40	83.70	<b>84.93</b>	<b>84.52</b>	70.49	7.92	73.56	<b>78.56</b>	<b>78.37</b>
Eyeglasses	Gender	98.20	85.47	98.38	<b>98.39</b>	<b>98.65</b>	96.24	76.89	96.85	<b>97.22</b>	<b>97.64</b>
Black Hair	Gender	84.92	61.00	85.19	<b>86.57</b>	<b>86.76</b>	75.47	22.04	75.69	<b>81.28</b>	<b>80.67</b>
<b>Average</b>	Gender	87.90	63.59	87.92	<b>88.89</b>	<b>88.93</b>	80.97	39.51	82.29	<b>84.10</b>	<b>83.86</b>

Table 5: Unbiased accuracy (%) with multiple bias attributes. For each target, our model only requires a single model, while Group DRO [25] should train separate models depending on the bias set.

Target	Blond Hair				Blurry			
	Unsupervised			Supervised Group DRO	Unsupervised			Supervised Group DRO
Biases	Baseline	LfF*	Ours		Baseline	LfF*	Ours	
Gender	80.42	84.89	90.18	<b>91.39</b>	73.05	76.70	<b>88.93</b>	87.05
Gender, Heavy Makeup	83.64	88.82	<b>91.90</b>	81.09	75.37	79.55	<b>89.09</b>	72.17
Gender, Wearing Lipstick	80.34	84.13	<b>91.63</b>	85.93	79.88	83.21	<b>89.79</b>	79.88
Gender, Young	78.39	81.21	<b>89.05</b>	87.96	72.97	77.77	<b>88.66</b>	85.39
Gender, No Beard	79.50	82.51	<b>89.92</b>	85.01	78.91	79.84	<b>84.06</b>	81.07
Gender, Wearing Necklace	79.25	81.03	<b>92.62</b>	92.26	71.80	78.07	<b>89.60</b>	85.33
Gender, Big Nose	81.18	84.10	90.58	<b>90.83</b>	71.89	77.11	<b>88.57</b>	87.11
Gender, Smiling	79.75	82.91	89.85	<b>91.73</b>	73.31	78.04	<b>89.32</b>	87.87
<b>Average</b>	80.29 $\pm$ 1.71	83.53 $\pm$ 2.64	<b>90.79 <math>\pm</math>1.29</b>	87.83 $\pm$ 4.10	74.88 $\pm$ 3.32	79.08 $\pm$ 2.06	<b>88.44 <math>\pm</math>1.98</b>	82.69 $\pm$ 5.50

work can be incorporated into the existing recognition models directly, without knowing the presence of dataset bias. Note that color classification with digit bias on Colored-MNIST or background place classification with object bias on Waterbirds are also qualified as unbiased settings, where our model gives consistent results.

**Multiple bias attributes** Thanks to the unsupervised nature of our method, we can simply evaluate our model on multi-bias scenarios, where multiple bias attributes exist in the dataset, without modification. Table 5 presents the unbiased results with multiple bias attributes using our method and Group DRO [25], where we additionally report the average and standard deviation over all bias sets to compare the overall effectiveness and robustness. We also present the results of LfF\*, a variant of LfF [24], introduced in Table 1. When trained on multiple bias attributes, the accuracy of Group DRO is sensitive to bias sets, while our method achieves stable and superior results for a variety of sets. This fact implies that inappropriate bias information can degrade the performance of the supervised debiasing method, requiring a thorough analysis to identify bias attributes. Note that our model is applicable to any bias sets without additional fine-tuning, while a supervised method

Table 6: Ablation results on our importance weighting scheme on the CelebA dataset with blond hair and gender for target and bias attributes, respectively, in terms of unbiased and worst-group accuracies (%).

Scale	Loss	Unbiased	Worst-group
		80.42	41.02
	✓	83.86	57.44
✓		89.08	76.55
✓	✓	<b>90.18</b>	<b>82.54</b>

should separately train their model for each set.

**Ablative results on importance weighting** We perform the ablative experiments on the CelebA dataset to analyze the effectiveness of our reweighting strategy. In Table 6, scale and loss indicates that only the scale  $N_k$  and the average loss  $\mathbb{E}_{(\mathbf{x}, y) \sim P_k}[\ell((\mathbf{x}, y); \theta)]$ , respectively, are taken into account to calculate the  $\omega_k$  for the  $k^{\text{th}}$  cluster in Eq. (6). Note that our ablative model with the loss factor only is closely related to [28]. Table 6 shows that combining both terms plays a crucial role for learning debiased representation while the scale factor is clearly more important. See our supplementary files for more comprehensive results with other attributes.

Table 7: Unbiased accuracy (%) with bias-unspecified settings. The results are the average of a set of unbiased accuracies, each of which additionally uses one of the other 25 unspecified attributes, in addition to the specified bias attribute (*gender*), as the bias attributes to define groups.

Target	Baseline	Ours	Group DRO
Blond Hair	79.13 $\pm$ 2.72	90.16 $\pm$ 3.19	<b>90.82</b> $\pm$ 2.76
Heavy Makeup	70.26 $\pm$ 3.84	<b>73.52</b> $\pm$ 3.86	71.57 $\pm$ 4.33
Young	77.56 $\pm$ 1.80	<b>81.31</b> $\pm$ 2.31	80.56 $\pm$ 2.09
Double Chin	62.56 $\pm$ 2.22	<b>81.71</b> $\pm$ 3.61	78.46 $\pm$ 3.37
Chubby	67.80 $\pm$ 2.77	<b>82.36</b> $\pm$ 3.55	79.91 $\pm$ 3.43
Wearing Hat	90.80 $\pm$ 4.01	<b>95.11</b> $\pm$ 3.10	94.71 $\pm$ 3.76
Oval Face	61.77 $\pm$ 1.80	<b>66.63</b> $\pm$ 1.63	65.35 $\pm$ 1.45
Pointy Nose	63.96 $\pm$ 1.42	<b>70.53</b> $\pm$ 1.52	70.16 $\pm$ 1.45

**Unspecified group shifts** To verify the robustness in another realistic scenario, we tested for unspecified group shifts, where the group information at test time is not fully provided during training. The specified bias attribute, which is used in group DRO during training, is fixed to *gender*. To evaluate the unbiased accuracy in this setting, we evaluate a set of unbiased accuracies, each of which additionally uses one of the other 25 unspecified bias attributes<sup>6</sup>, in addition to *gender*, as the bias attributes to define groups, respectively. We finally report the average and standard deviation of the set of unbiased accuracies. Table 7 clearly shows that our model provides better results than Group DRO in the bias-unspecified setting. This implies that, although Group DRO can handle group shifts well within the simplex of the specified group distributions, it can suffer from worst-case generalization for unspecified group shifts. Note that our method does not differentiate specified and unspecified group shifts, since it does not use any information of bias.

**Sensitivity analysis on the number of clusters** We conduct ablation study on the number of clusters for clustering on the feature embedding space to obtain bias pseudo-attributes on the CelebA dataset. We set *gender* as the bias attribute and evaluate the unbiased accuracy with several target attributes. Figure 2 presents that the results are stable over a wide range of the number of clusters, which is almost saturated when  $K \geq 4$ .

**Feature visualization** Figure 3 illustrates the t-SNE visualization of instance embeddings using baseline (left) and ours (right) on the CelebA dataset with hair color (*blond hair*) classification. Plus (+) and circle (●) marker types denote heavy makeup and no-makeup of the target attribute,

<sup>6</sup>Unspecified bias attribute denotes the bias attribute that is not specified during training but used to define groups for evaluation at test time. We filtered 26 out of 39 attributes as in Section 4.4, and excluded the target attribute.

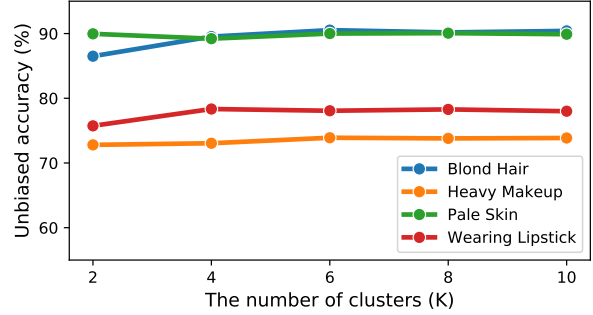


Figure 2: Sensitivity analysis on the number of clusters in our framework on the CelebA dataset.

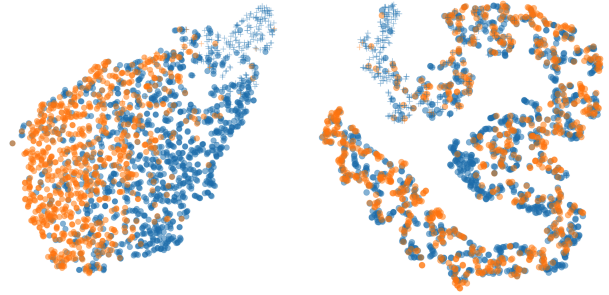


Figure 3: T-SNE plots of feature embeddings using baseline (left) and ours (right) trained to classify *blond hair* (marker type) as the target attribute with *gender* (color) as the bias attribute. Our framework helps to confuse samples which have the same target attributes but different bias attributes.

respectively, while blue and orange colors indicate female and male of the bias attribute, respectively. We observe that our model helps to confuse the examples on the feature embedding space among different groups within the same class, which is desirable for debiasing.

## 5. Conclusion

We presented a generic debiasing framework in an unsupervised way. We observe that the examples which have the same attribute values are closely located in the feature embedding space. Based on our empirical observation, we claimed that it is possible to identify the pseudo-attributes by taking advantage of the embedding results even without the attribute supervision. Inspired by this fact, we introduced a novel cluster-based reweighting strategy for learning debiased representation. We demonstrated the effectiveness of our method on multiple standard benchmarks, which is even as competitive as the supervised debiasing method. We also conducted a thorough analysis of our framework in many realistic scenarios, where our model provides substantial gain consistently.



## References

- [1] Hyojin Bahng, Sanghyuk Chun, Sangdoo Yun, Jaegul Choo, and Seong Joon Oh. Learning de-biased representations with biased representations. In *ICML*, 2020. 1, 2, 5
- [2] Aharon Ben-Tal, Dick Den Hertog, Anja De Waegenare, Bertrand Melenberg, and Gijs Rennen. Robust solutions of optimization problems affected by uncertain probabilities. *Management Science*, 59(2):341–357, 2013. 1, 2, 3
- [3] Remi Cadene, Corentin Dancette, Matthieu Cord, Devi Parikh, et al. Rubi: Reducing unimodal biases for visual question answering. In *NeurIPS*, 2019. 1, 2
- [4] Fabio M Carlucci, Antonio D’Innocente, Silvia Bucci, Barbara Caputo, and Tatiana Tommasi. Domain generalization by solving jigsaw puzzles. In *CVPR*, 2019. 2
- [5] Alexandra Chouldechova and Aaron Roth. The frontiers of fairness in machine learning. *arXiv preprint arXiv:1810.08810*, 2018. 2
- [6] Christopher Clark, Mark Yatskar, and Luke Zettlemoyer. Don’t take the easy way out: Ensemble based methods for avoiding known dataset biases. In *EMNLP*, 2019. 2
- [7] Michele Donini, Luca Oneto, Shai Ben-David, John S Shawe-Taylor, and Massimiliano Pontil. Empirical risk minimization under fairness constraints. In *NIPS*, 2018. 2
- [8] John Duchi, Peter Glynn, and Hongseok Namkoong. Statistics of robust optimization: A generalized empirical likelihood approach. *arXiv preprint arXiv:1610.03425*, 2016. 2, 3
- [9] John Duchi, Tatsunori Hashimoto, and Hongseok Namkoong. Distributionally robust losses for latent covariate mixtures. *arXiv preprint arXiv:2007.13982*, 2020. 2, 3
- [10] Rui Gao, Xi Chen, and Anton J Kleywegt. Wasserstein distributional robustness and regularization in statistical learning. *arXiv preprint arXiv:1712.06050*, 2017. 2
- [11] Robert Geirhos, Jörn-Henrik Jacobsen, Claudio Michaelis, Richard Zemel, Wieland Brendel, Matthias Bethge, and Felix A Wichmann. Shortcut learning in deep neural networks. *arXiv preprint arXiv:2004.07780*, 2020. 1
- [12] Robert Geirhos, Patricia Rubisch, Claudio Michaelis, Matthias Bethge, Felix A Wichmann, and Wieland Brendel. Imagenet-trained cnns are biased towards texture; increasing shape bias improves accuracy and robustness. In *ICLR*, 2019. 2
- [13] Lisa Anne Hendricks, Kaylee Burns, Kate Saenko, Trevor Darrell, and Anna Rohrbach. Women also snowboard: Overcoming bias in captioning models. In *ECCV*, 2018. 1
- [14] Weihua Hu, Gang Niu, Issei Sato, and Masashi Sugiyama. Does distributionally robust supervised learning give robust classifiers? In *ICML*, 2018. 2, 3
- [15] Justin Johnson, Bharath Hariharan, Laurens van der Maaten, Li Fei-Fei, C Lawrence Zitnick, and Ross Girshick. Clevr: A diagnostic dataset for compositional language and elementary visual reasoning. In *CVPR*, 2017. 2
- [16] Johannes Kirschner, Ilija Bogunovic, Stefanie Jegelka, and Andreas Krause. Distributionally robust bayesian optimization. In *AISTATS*, 2020. 2, 3
- [17] Da Li, Yongxin Yang, Yi-Zhe Song, and Timothy M Hospedales. Deeper, broader and artier domain generalization. In *ICCV*, 2017. 1, 2
- [18] Tian Li, Maziar Sanjabi, Ahmad Beirami, and Virginia Smith. Fair resource allocation in federated learning. *arXiv preprint arXiv:1905.10497*, 2019. 2
- [19] Yingwei Li, Yi Li, and Nuno Vasconcelos. Resound: Towards action recognition without representation bias. In *ECCV*, 2018. 2
- [20] Yi Li and Nuno Vasconcelos. Repair: Removing representation bias by dataset resampling. In *CVPR*, 2019. 1, 2, 5
- [21] Ziwei Liu, Ping Luo, Xiaogang Wang, and Xiaoou Tang. Deep learning face attributes in the wild. In *ICCV*, 2015. 5
- [22] Ilya Loshchilov and Frank Hutter. Sgdr: Stochastic gradient descent with warm restarts. In *ICLR*, 2017. 5
- [23] Mehryar Mohri, Gary Sivek, and Ananda Theertha Suresh. Agnostic federated learning. *arXiv preprint arXiv:1902.00146*, 2019. 2
- [24] Junhyun Nam, Hyuntak Cha, Sungsoo Ahn, Jaeho Lee, and Jinwoo Shin. Learning from failure: Training debiased classifier from biased classifier. In *NeurIPS*, 2020. 1, 2, 3, 5, 6, 7
- [25] Shiori Sagawa, Pang Wei Koh, Tatsunori B Hashimoto, and Percy Liang. Distributionally robust neural networks for group shifts: On the importance of regularization for worst-case generalization. In *ICLR*, 2020. 1, 2, 3, 4, 5, 6, 7
- [26] Shiori Sagawa, Aditi Raghunathan, Pang Wei Koh, and Percy Liang. An investigation of why overparameterization exacerbates spurious correlations. In *ICML*, 2020. 3
- [27] Seonguk Seo, Yumin Suh, Dongwan Kim, Geeho Kim, Jongwoo Han, and Bohyung Han. Learning to optimize domain specific normalization for domain generalization. In *ECCV*, 2020. 2
- [28] Nimit Sohoni, Jared Dunnmon, Geoffrey Angus, Albert Gu, and Christopher Ré. No subclass left behind: Fine-grained robustness in coarse-grained classification problems. In *NeurIPS*, 2020. 2, 3, 4, 7
- [29] Antonio Torralba and Alexei A Efros. Unbiased look at dataset bias. In *CVPR*, 2011. 2
- [30] Catherine Wah, Steve Branson, Peter Welinder, Pietro Perona, and Serge Belongie. The caltech-ucsd birds-200-2011 dataset. 2011. 5
- [31] Angelina Wang, Arvind Narayanan, and Olga Russakovsky. REVISE: A tool for measuring and mitigating bias in visual datasets. In *ECCV*, 2020. 2
- [32] Haohan Wang, Zexue He, Zachary L. Lipton, and Eric P. Xing. Learning robust representations by projecting superficial statistics out. In *ICLR*, 2019. 1
- [33] Mei Wang, Weihong Deng, Jiani Hu, Xunqiang Tao, and Yaohai Huang. Racial faces in the wild: Reducing racial bias by information maximization adaptation network. In *ICCV*, 2019. 2
- [34] Tianlu Wang, Jieyu Zhao, Mark Yatskar, Kai-Wei Chang, and Vicente Ordonez. Balanced datasets are not enough: Estimating and mitigating gender bias in deep image representations. In *ICCV*, 2019. 2

- [35] Rich Zemel, Yu Wu, Kevin Swersky, Toni Pitassi, and Cynthia Dwork. Learning fair representations. In *ICML*, 2013. [1](#), [2](#)
- [36] Marvin Zhang, Henrik Marklund, Abhishek Gupta, Sergey Levine, and Chelsea Finn. Adaptive risk minimization: A meta-learning approach for tackling group shift. *arXiv preprint arXiv:2007.02931*, 2020. [1](#)
- [37] Yi Zhang and Jitao Sang. Towards accuracy-fairness paradox: Adversarial example-based data augmentation for visual debiasing. *arXiv preprint arXiv:2007.13632*, 2020. [2](#)
- [38] Bolei Zhou, Agata Lapedriza, Aditya Khosla, Aude Oliva, and Antonio Torralba. Places: A 10 million image database for scene recognition. *TPAMI*, 40(6):1452–1464, 2017. [5](#)